



## Science Arts & Métiers (SAM)

is an open access repository that collects the work of Arts et Métiers ParisTech researchers and makes it freely available over the web where possible.

This is an author-deposited version published in: <http://sam.ensam.eu>  
Handle ID: [.http://hdl.handle.net/null](http://hdl.handle.net/null)

### To cite this version :

Maxence BIGERELLE, Alain IOST - Statistical artefacts in the determination of the fractal dimension by the slit island method - Engineering Fracture Mechanics - Vol. 71, n°7-8, p.1081-1105 - 2004

Any correspondence concerning this service should be sent to the repository

Administrator : [archiveouverte@ensam.eu](mailto:archiveouverte@ensam.eu)

# Statistical artefacts in the determination of the fractal dimension by the slit island method

Maxence Bigerelle, Alain Iost \*

*Equipe ENSAM "Surfaces et Interfaces", Laboratoire de Mee'tallurgie Physique et Gee'nie des Matee'riaux, CNRS UMR 8517, 8 Boulevard Louis XIV, 59046 Lille Cedex, France*

## Abstract

This paper comments upon some statistical aspects of the slit island method which is widely used to calculate the fractal dimension of fractured surfaces or of materials' features like grain geometry. If a noise is introduced when measuring areas and perimeters of the islands (experimental errors), it is shown that errors are made in the calculation of the fractal dimension and more than a false analytical relation between a physical process parameter and the fractal dimension can be found. Moreover, positive or negative correlation with the same physical process parameter can be obtained whether the regression is performed by plotting the variation of the noisy area versus the noisy perimeter of the considered islands or vice versa. Monte-Carlo simulations confirm the analytical relations obtained under statistical considerations.

*Keywords:* Fractal dimension; Slit island method; Monte-Carlo simulation; Statistics; Artefact measurement

## 1. Introduction

Since Mandelbrot's [1,2] pioneering work from the fractal geometry has been extensively applied to describe various irregular phenomena in nature. As it was shown that real surfaces such as fractured surfaces in materials are fractal [3–5] i.e. self-similar (or self-affine) over a wide range of scales, extensive work was done to correlate the fractal dimension of the surfaces with mechanical properties such as impact energy [6], fracture toughness [7], fatigue crack propagation [8]... The experimental results show that a general conclusion cannot easily be drawn [9]: some studies report a positive variation of fracture toughness along with the fractal dimension [6,10–13], and others a negative one [14–17]. To other researchers, there is either no correlation [18–20] or the fractal dimension of the fractured surfaces is a universal constant [21].

One of the major reasons to this discrepancy is related to the method used to calculate the fractal dimension. Different methods (Slit Island [2,14], Vertical Section [22], Richardson [23], Minkowski Sausage

\* Corresponding author. Tel.: +33-3-2062-2233; fax: +33-3-2062-2957.

*E-mail address:* [alain.iost@lille.ensam.fr](mailto:alain.iost@lille.ensam.fr) (A. Iost).

[24], Box Counting [25,26], Spectrum [26,27]. . .) applied onto the same fractured surface can give different fractal dimensions. If some discrepancies can easily be understood by the experimental limits and material properties (length of the recorded profile, textured material, structural heterogeneity. . .), others seem related to the method used to calculate the fractal dimension.

The aim of this paper is to analyse the slit island method (SIM), one of the most widely used to determine the fractal dimension of fractured surfaces,  $\Delta$ , and to show that, in some cases, the origin of positive or negative correlation between fractal dimension and mechanical properties may be caused by statistical artefacts related to noise measurement.

## 2. The slit island method

For Euclidean forms, the ratio between perimeter ( $P$ ) and the square root of the area ( $A$ ) is an  $a$ -dimensional constant (e.g.  $2\sqrt{\pi}$  for a circle). This ratio, known as the shape factor, is extensively used in quantitative metallography. However for fractal shapes such as cloud [28] mammal's cerebral cortex [29], human lung [30], basins of attraction [31], this ratio is not constant but depends on the observation scale. From these observations, Mandelbrot [2] derived a perimeter–area relationship which when applied to fractured surfaces is called the “Slit Island Method”. Mandelbrot, Passoja and Paullay first applied the method in 1984 [14] when studying the fracture toughness of 300-grade maraging steel and correlated the fractal dimension with the impact energy. It consists in electroplating and mounting in resin the fractured specimen in order to ensure edge retention. The specimen is then polished parallel to the plane of fracture in successive stages. At varying intervals of grinding time corresponding to a few micrometers removal, the sample is observed in optic or scanning electron microscopy. Islands of the material first merged in the resin and grow in size as polishing progresses. The islands contain “lake within islands and islands within lakes”. Mandelbrot et al. [14] include the former and neglect the latter, but different solutions are adopted by other authors [32,33].

This method was founded on the following statements:

- (i) When islands are derived from initial self-affine fractal surface of dimension  $\Delta_s$  by sectioning with a plane, their coastlines are self-similar fractals with dimension  $\Delta = \Delta_s - 1$ .
- (ii) The relation between perimeter and area is given by Eq. (1):

$$R(\eta) = \frac{[P(\eta)]^{1/\Delta}}{\sqrt{A(\eta)}} \quad (1)$$

where  $R(\eta)$  is a constant which depends on the choice of the yardstick length,  $\eta$ , used to measure the length along the walking path.

This equation is only true for self-similar islands [2,14,34,35] whose perimeter and area are measured in the same way.

- (iii) When the graph of  $\log(\textit{Perimeter})$  versus  $\log(\textit{Area})$  is rectilinear, the fractal dimension is deduced from the slope.

In spite of a few serious problems with the method [3,19,32,34–39] a lot of papers have been published over the past 10 years concerning the relationship between mechanical properties and the fractal dimension calculated by the SIM. The most surprising result was an inversion relation between fractal dimension and toughness for the same material [6,14] that allows us to investigate if all the criticisms against the method were not due to some statistical errors. For this reason, in the following paragraph, we shall consider only

the influence of an experimental noise on the validity of the calculation of the fractal dimension and the related correlation with mechanical properties.

### 3. Statistical aspect of the area–perimeter relation

The perimeter area relation Eq. (1) could be written in the following form:

$$\log(A) = \frac{2}{D} \log(P) + \beta \quad (2)$$

and the fractal dimension is obtained from the slope of the plot of  $\log(\text{Area})$  versus  $\log(\text{Perimeter})$ .

The precision depends on the density probability of both the area and the perimeter. Different shapes obtained by the SIM on samples from the same material get an intrinsic variation. The distribution was defined by Mandelbrot as a stochastic self-similarity [2], which means that both the perimeter and the area measurements get a probability density function (PDF) (even if this PDF is unknown) and as a consequence an intrinsic variation.

#### 3.1. Determination of the uncertainty

To apply SIM, all islands must be measured with the same yardstick length  $\eta$  [2,40].

Let  $n$ , be the number of islands, respectively  $P_i$  the perimeter and  $A_i$  the area of the  $i$ th island,  $\alpha = 2/D$ , the slope of the linear plot of  $\log(A) = f[\log(P)]$  and  $a$  its estimation.

According to Eq. (1), the fractal dimension is estimated by linear regression of the relation:

$$\log(A) = \frac{2}{D} \log(P) + \beta + \varepsilon \quad (3)$$

where  $\beta$  is the intercept at the origin, and  $\varepsilon$  a random vector that represents the noise on the area measurement.

If  $s_A$  is the unbiased estimation of the residual standard deviation then:

$$s_A^2 = \frac{\sum_{i=1}^n (\log A_i^{\text{Model}} - \log A_i^{\text{Exp.}})^2}{n - 2} \quad (4)$$

Given the following hypotheses:

**Hypothesis 1.**  $\varepsilon$  obeys a Gaussian law meaning that the measure of the area obeys a lognormal law.

**Hypothesis 2.** The residual variance is constant independently of the value of  $\log(P)$  (homoscedasticity).

**Hypothesis 3.** The  $\varepsilon$  autocorrelation function equals zero.

Then the variable  $t = (a - \alpha)/s_a$  obeys here a Student law with  $n - 2$  degrees of freedom and the  $a$  variance (variance of the slope given by Eq. (3)) is given by:

$$s_a^2 = \frac{s_A^2}{\sum_{i=1}^n (\log P_i - \log \bar{P})^2} \quad (5)$$

where  $\bar{P}$  is the mean of the island perimeter:  $\sum_{i=1}^n (\log P_i - \log \bar{P})^2 = (n - 1)\text{Var}(\log P)$ .

If the additional hypotheses are considered:

**Hypothesis 4a.**  $\log(P)$  obeys a uniform law.

Then if  $P_{\min}$  and  $P_{\max}$  are respectively the minimum and the maximum of the perimeter range of all recorded islands, then:

$$\text{Var}(\log P) = \frac{(\log P_{\max} - \log P_{\min})^2}{12}$$

and therefore

$$\sigma_x = \sqrt{s_x^2} = \frac{s_\varepsilon \sqrt{12}}{(\log P_{\max} - \log P_{\min}) \sqrt{n-1}}$$

where  $s_\varepsilon$  is the standard deviation of the noise  $\varepsilon$  given by Eq. (3).

Taken  $\delta_\beta$  the required accuracy on the determination of the slope (at  $\beta = 95\%$  confidence interval):

$$\frac{2t_{n-2} s_\varepsilon \sqrt{12}}{\Delta_P \sqrt{n-1}} \leq \delta_\beta \quad (6)$$

with  $\Delta_P = \log \frac{P_{\max}}{P_{\min}}$ , the number of decades used for the determination of the perimeter.

**Hypothesis 5.** The number of islands is higher than 30.

Then the Student law converges towards a Laplace–Gauss one and  $t_{n>30} \approx 2$ , then:

$$\frac{4s_\varepsilon \sqrt{12}}{\Delta_P \sqrt{n}} \leq \delta_\beta \quad (7)$$

**Hypothesis 4b.** The area  $A$  obeys a uniform PDF.

Instead of using Eq. (3), the regression to calculate  $\Delta$  is carried out with Eq. (8):

$$\log(P) = \frac{\Delta}{2} \log(A) + \beta' + \varepsilon' \quad (8)$$

where  $\varepsilon'$  represents the noise on the perimeter measurement and  $\beta'$  the intercept.

With the same reasoning as above the variance for the fractal dimension is:

$$\frac{4s_{\varepsilon'} \sqrt{12}}{\Delta_A \sqrt{n}} \leq \delta_{\beta'} \quad (9)$$

where  $\Delta_A$  is the number of decades used for the determination of the area ( $\Delta_A = \log \frac{A_{\max}}{A_{\min}}$ ).

The following statistical considerations can be stated:

- (i) The island-recorded area must cover a broad range of sizes since the islands obtained from experimental images are random variables whose scattering depends on the recording process. If the experimental range used to calculate the fractal dimension is not large enough, so the noise due to the error during measurement is too large and no correlation can be found. The SIM does not apply, but perhaps the Richardson method [41] can give more reliable results.
- (ii) The precision in the determination of the fractal dimension is better if the number of islands considered is high.
- (iii) To double the precision in the determination of the fractal dimension we must increase fourfold the number of islands or double the number of decades.

Table 1

Literature results of impact or fracture toughness measurements related to the fractal dimension

Author	Reference	Relation	$\Delta_P$	$\Delta_A$	$s_P$	$s_A$	$n_{isl}$	$\Delta_{min}$	$\Delta_{max}$	$\Delta_A$	$n_A$	Corr.
Mandelbrot	[14]	$A = f(P)$	3	4	0.15	0.2	48	1.1	1.3	0.2	6	-
Su	[15]	$P = f(A)$	0.6	0.6	0.1	0.05	31	1.2	1.8	0.6	5	-
Pande	[18]	$P = f(A)$	1	2	0.1	0.15	20	1.41	1.46	0.06	5	====
<i>Wang (Fat)</i>	<i>[8]</i>	$P = f(A)$	2.5	4	0.07	0.17	44	1.1	1.22	0.12	9	+++
Ray	[6]	$A = f(P)$	2	3	0.2	0.2	15	1	1.52	0.52	5	+++
Su	[44]	$P = f(A)$	0.7	1.1	0.05	0.04	41	1.15	1.37	0.22	4	+++
Mecholski	[11]	$A = f(P)$	1.4	2.2	0.22	0.21	27	1.04	1.2	0.16	11	+++
Pande	[45]	$A = f(P)$	1.4	2.2	0.1	0.16	37	1.32	1.32		1	====
Richards	[19]	$A = f(P)$	2	3	0.07	0.27	23	1.77	1.91	0.14	4	====

$\Delta_P$ : Number of decades of perimeter,  $\Delta_A$ : Number of decades of area,  $s_P$ : Standard deviation of the perimeter measure (in log),  $s_A$ : Standard deviation of the area measure (in log),  $n_{isl}$ : Number of islands,  $\Delta_{min}$ : Lower fractal dimension,  $\Delta_{max}$ : Higher fractal dimension,  $\Delta_A$ : Range variation of  $\Delta$ ,  $n_A$ : Number of samples used to quantify the relation.

+++ : Means positive correlation, ==== : No correlation, - : Negative correlation. (Italic: fatigue crack profiles and relation between  $\Delta K$ th and fractal dimension).

### 3.2. Area versus perimeter or perimeter versus area?

Positive or negative fractal dimension values were found by Ray et Mandal [6] using respectively perimeter or area in the abscissa for the log-log plot. In the same way, the analysis of the results coming from the literature shows that the positive or negative correlation between  $\Delta$  and the mechanical properties (or the lack of correlation) depends on the abscissa ( $\log P$  or  $\log A$ ) chosen for the regression (Table 1) [42]. These results obviously question the validity of the Slit Island Method. To answer these questions we first studied the precision in the determination of the fractal dimension related to the two types of representation.

#### 3.2.1. Perimeter versus area representation

With Hypotheses 1, 2, 3 and 5, when  $\Delta$  is deduced from Eq. (8), the density function of the residual obeys a Gaussian law as well as  $\alpha$  (from Eq. (3)) but not  $\Delta$  since the change of variable  $\alpha = 2/\Delta$  destroys the normality of the estimation of the fractal dimension.

If  $\Delta_{P=f(A)}$  and  $\Delta_{A=f(P)}$  are the fractal dimensions obtained respectively by Eqs. (8) and (3), we will prove that  $E(\Delta_{P=f(A)})$  is different from  $E(\Delta_{A=f(P)})$  where  $E(X)$  is the expectation of the variable  $X$ .

*Demonstration:* If  $\alpha$  obeys a Gaussian law then

$$x = \frac{\frac{2}{\Delta_{A=f(P)}} - \bar{\alpha}}{\sigma_\alpha}$$

is a reduced centred Gaussian and then:

$$\Delta_{A=f(P)} = \frac{2}{\bar{\alpha}} \frac{1}{1 + \frac{\sigma_\alpha}{\bar{\alpha}} x}$$

Developing in function of the  $x$  rising order:

$$\Delta_{A=f(P)} = \frac{2}{\bar{\alpha}} \left[ 1 - \frac{\sigma_\alpha}{\bar{\alpha}} x + \left( \frac{\sigma_\alpha}{\bar{\alpha}} \right)^2 x^2 - \left( \frac{\sigma_\alpha}{\bar{\alpha}} \right)^3 x^3 + \dots \right]$$

and calculating the mean  $E[\Delta_{A=f(P)}]$  from  $\Delta_{A=f(P)}$ :

$$E[\Delta_{A=f(P)}] = \frac{2}{\bar{\alpha}} \left[ 1 + \left( \frac{\sigma_x}{\bar{\alpha}} \right)^2 \mu_{P=f(A)}^2 + \left( \frac{\sigma_x}{\bar{\alpha}} \right)^4 \mu_{P=f(A)}^4 + \dots \right] \quad (10)$$

where  $\mu_{P=f(A)}^N$  is the moment of order  $N$  of the fractal dimension calculated by Eq. (8). The expected value exists only if the preceding series converges and then

$$\lim_{i \rightarrow \infty} \left( \frac{\mu_{P=f(A)}^{2i+2}}{\mu_{P=f(A)}^{2i}} \right) < 1$$

However, from Eq. (10),

$$\lim_{i \rightarrow \infty} \left( \frac{\mu_{P=f(A)}^{2i+2}}{\mu_{P=f(A)}^{2i}} \right) > 1$$

and then the series diverges and the fractal dimension cannot be calculated by means of Eq. (3) (see Appendix A). This result is understandable since the probability is not nul to obtain a zero slope by using Eq. (3) and then an infinite fractal dimension. However, it is possible to state positively that if the experimental noise is low then  $\alpha > 0$ , meaning that the Gaussian law for  $\alpha$  is truncated. With the assumption that  $\alpha \in [\bar{\alpha} - T, \bar{\alpha} + T]$  with  $\bar{\alpha} - T \gg 0$ ,

$$\lim_{i \rightarrow \infty} \left( \frac{\mu_{P=f(A)}^{2i+2}}{\mu_{P=f(A)}^{2i}} \right) = T^2 \quad \text{and} \quad E[\Delta_{A=f(P)}]$$

converges if  $(\frac{\sigma_x}{\bar{\alpha}})^2 T^2 < 1$ . More if  $\sigma_x/\bar{\alpha}$  is low:

$$E[\Delta_{A=f(P)}] \approx \frac{2}{\bar{\alpha}} \left[ 1 + \left( \frac{\sigma_x}{\bar{\alpha}} \right)^2 \mu_{P=f(A)}^2 \right] \quad (11)$$

and it appears a positive bias  $(\frac{\sigma_x}{\bar{\alpha}})^2 \mu_{P=f(A)}^2$ .

If  $T$  is high enough (the  $\alpha$  Gaussian is weakly truncated) then  $\mu_{P=f(A)}^2 \approx 1$ . If  $\bar{\alpha}$  is perfectly determined then  $\bar{\alpha} = 2/\Delta$ , and the following fundamental equation can be obtained:

$$E[\Delta_{A=f(P)}] \approx \Delta \left[ 1 + \left( \frac{\sigma_x \Delta}{2} \right)^2 \right] \quad (12)$$

This equation involves the following physical consequences:

- (i) If the residual scatter for the linear plot of  $\log(\text{Area})$  versus  $\log(\text{Perimeter})$  is low, then  $E[\Delta_{A=f(P)}] \approx 2/\bar{\alpha}$  and therefore there is no difference for the fractal dimension calculated by means of Eq. (8) or Eq. (3).
- (ii) The fractal dimension is especially overestimated when the true fractal dimension is high.
- (iii) The fractal dimension is especially overestimated when the experimental noise rises. Statistical biases are often reported in material experimental measurements that lead to misinterpretations when neglected [43].
- (iv) Suppose that the real unknown fractal dimension  $\Delta$  is unchanged, then from Eq. (12):
  - As  $\sigma_x^2 \propto 1/n$ , when the number of recorded islands rises, the estimated fractal dimension diminishes even if the true value is constant.
  - As  $\sigma_x^2 \propto s_e^2$ , the calculated fractal dimension rises with the residual variance.
  - As  $\sigma_x^2 \propto 1/\Delta_p$ , the fractal dimension rises in proportion with the number of decades.

From these relations it is clear that if a physical process does not change the fractal dimension, but modifies the image morphology with a monotonous law (fewer islands, different noise levels) a correlation between the fractal dimension and the physical process can be erroneously stated.

This statistical artefact may be at the origin of some correlations between mechanical properties (MP) and the fractal dimension reported in literature. If the fractal dimension of the fractured surface does not depend on MP, Eq. (3) implies a negative correlation between fractal dimension and MP if:

- (i) The number of recorded islands rises as MP rises.
- (ii) The area standard deviation decreases with MP.
- (iii) The number of decades rises with MP.

On the other hand provided the Hypotheses 1–3 are respected, the average calculated fractal dimension tends toward the theoretical one when Eq. (8) is used.

### 3.2.2. Area versus perimeter representation

Different fractal dimensions are obtained when using the regression of  $\log(\text{Area})$  versus  $\log(\text{Perimeter})$  or  $\log(\text{Perimeter})$  versus  $\log(\text{Area})$ . In fact, the least square theory leads to the following equations without any prior hypotheses related to the experimental data:

$$\Delta_{P=f(A)} = 2r \frac{\sigma_P}{\sigma_A} \quad (13)$$

$$\Delta_{A=f(P)} = 2 \frac{1}{r} \frac{\sigma_P}{\sigma_A} \quad (14)$$

where  $\sigma_P$  and  $\sigma_A$  are respectively the standard deviation for  $\log(\text{Perimeter})$  and  $\log(\text{Area})$  and  $r$  the correlation coefficient. From the above equations it can be stated that:

$$\frac{\Delta_{P=f(A)}}{\Delta_{A=f(P)}} = r^2 \quad (15)$$

As a consequence the same fractal dimension is obtained for the two types of representation only if the mathematical relationship is perfect i.e. the coefficient of correlation is  $r = 1$ . As this coefficient does not depend on the regression, the difference between the fractal dimension calculated by means of Eqs. (3) and (8) rises with the scattering of the data. It is usual to take as abscissa the variable  $X$  which is controlled by the experimenter, and as ordinate the answer  $Y$  (dependent variable that contains experimental noise). For the Richardson plots the unambiguous abscissa is the yardstick length that is a deterministic value and  $Y$  the measured perimeter that is a stochastic value. For the slit island method there is no a priori reason for choosing perimeter or area in ordinate.

Nevertheless Eq. (15) requires the knowledge of the regression coefficient, which depends on the experimental data, and it is necessary to evaluate the discrepancy.

### 3.2.3. Probabilistic behaviour

Assuming that the measure of the area is obtained precisely,  $\Delta_{P=f(A)}$  is calculated such as

$$\log(P) = \gamma \log(A) + \beta' + \varepsilon', \quad \text{with } \gamma = \frac{\Delta_{P=f(A)}}{2}$$

As

$$r^2 = 1 - \frac{s_{\varepsilon'}^2}{\text{Var } \log P} \quad \text{with } \frac{\Delta_{P=f(A)}}{\Delta_{A=f(P)}} = r^2$$



where  $s_{e'}$  is the standard deviation of residual  $e'$  (such that  $E(s_{e'}) = 0$  where  $E(x)$  is the mean of  $x$ ).  $\text{Var} \log(P)$  can be split up with a modelled and a residual variance  $\text{Var} \log P = \text{Var} \log P|_{\text{mod}} + s_{e'}^2$ .  $\log P|_{\text{mod}} = \gamma \log A + b$  induces  $\text{Var} \log P|_{\text{mod}} = \gamma^2 \text{Var} \log A$  (supposing  $\text{cov}(\gamma, b) \approx 0$ ) and if  $\log A$  obeys a uniform law with interval  $\Delta_A$ , then  $\text{Var} \log P|_{\text{mod}} = \gamma^2 \frac{\Delta_A^2}{12}$ , and as a consequence:

$$\frac{\Delta_{P=f(A)}}{\Delta_{A=f(P)}} \cong 1 - \frac{s_{e'}^2}{s_{e'}^2 + \gamma^2 \frac{\Delta_A^2}{12}} \quad (16)$$

This formula entails the following remarks:

- (i)  $\Delta_{A=f(P)} > \Delta_{P=f(A)}$  the fractal dimension calculated by Eq. (3) is always higher than that calculated by Eq. (8).
- (ii) The difference between these two methods decreases when:
  - The fractal dimension rises because  $\gamma = \Delta/2$ .
  - The number of decade rises.
  - The noise in the perimeter measurement decreases.

### 3.2.4. Statistical behaviour

The above considerations are only probabilistic, and sampling is not considered. Because of the statistical bias, results can be different from the solutions of Eq. (16). To test whether the experimental data match the model corresponding to Eq. (16), an attempt to theoretical approach has been performed, but no simplification for the density function was obtained (the moment is not defined for  $\Delta_{A=f(P)}$ , then the  $r^2$  density function cannot be simplified). For this reason, we proceeded a Monte-Carlo simulation as follows on purpose to analyse Eq. (16):

Let  $\aleph_{a,s,\Delta_A,k,n,t}$ , be the space of configurations,  $\gamma \in \{0.5, 0.6, \dots, 2\}$ ;  $s_{e'} \in \{0.01, 0.02, \dots, 0.5\}$ ;  $\Delta_A \in \{0.5, 0.1, \dots, 5\}$ ; and  $A \in \{\frac{0}{n}\Delta_A, \frac{1}{n}\Delta_A, \frac{2}{n}\Delta_A, \dots, \frac{k}{n}\Delta_A, \dots, \frac{n}{n}\Delta_A\}$  where  $\Delta_A$  is the decade number in the area measurement,  $n$  is the number of data used for the regression analysis and  $s_{e'}$  the standard deviation of the noise in the area measurement (in log). This set of configurations is based on experimental values found in literature for the SIM.

The relation  $\log(P) = a \log(A) + e'$  is simulated 100 times, where error  $e'$  simulated by the Cox and Muller transformation obeys a Gaussian law with zero mean and standard deviation  $s_{e'}$ .

The following notations are adopted: Let  $\Pi_{a=\theta_a, s=\theta_s, \Delta_A=\theta_{\Delta_A}, k=\theta_k, n=\theta_n, t=\theta_t}$  be an element of  $\aleph_{a,s,\Delta_A,k,n,t}$ , and  $(A_{a=\theta_a, s=\theta_s, \Delta_A=\theta_{\Delta_A}, k=\theta_k, n=\theta_n, t=\theta_t}, P_{a=\theta_a, s=\theta_s, \Delta_A=\theta_{\Delta_A}, k=\theta_k, n=\theta_n, t=\theta_t})$  the co-ordinates of a simulated point with  $t$  the  $t$ th simulation.

The index  $\theta$  will be substituted by  $\theta = \bullet$  when the pair is considered for all discrete values  $\theta$  of  $\aleph$ .

In the same way  $f(\Pi_{a=\theta_a, s=\theta_s, \Delta_A=\theta_{\Delta_A}, k=\theta_k, n=\theta_n, t=\theta_t})$  is a statistic on the space  $a = \theta_a, s = \theta_s, \Delta_A = \theta_{\Delta_A}, k = \theta_k, n = \theta_n, t = \theta_t$ , and  $f(\Pi_{a,s,\Delta_A,k,n,t})$  a statistic built on  $\aleph$  and with value on  $\aleph$ .

*Examples:*

- $\Pi_{a=\theta_a, s=\theta_s, \Delta_A=\theta_{\Delta_A}, k=\theta_k, n=100, t=\bullet}$  is the space of 100 pairs simulated with  $a = \theta_a, s = \theta_s, \Delta_A = \theta_{\Delta_A}, k = \theta_k$ , and the associated mean is  $E[\Pi_{a=\theta_a, s=\theta_s, \Delta_A=\theta_{\Delta_A}, k=\theta_k, n=100, t=\bullet}]$ .
- $E[\Pi_{a,s,\Delta_A,k,n=100,t=\bullet}]$  is the mean of the area and perimeter calculated for 100 Monte-Carlo simulations for each value of the parameters  $a, s, \Delta_A, k$  members of  $\aleph$ .

We first verified Eq. (16) by simulating  $\Pi_{a,s,\Delta_A,k,n=100,t}$  and the calculation of the regression slopes obtained by the least square method for Eqs. (3) and (8). The mean

$$E \left[ \frac{\Delta_{a,s,\Delta_A,k,n=100,t=\bullet}^{P=f(A)}}{\Delta_{a,s,\Delta_A,k,n=100,t=\bullet}^{A=f(P)}} \right]$$

is then compared with Eq. (16). Fig. 1 shows the ratio of fractal dimension  $\Delta_{P=f(A)}/\Delta_{A=f(P)}$  in relation with the experimental noise standard deviation for two ranges of sizes: 0.5 decade (Fig. 1a) and five decades for the area measurement (Fig. 1b) and six different theoretical fractal dimensions varying between 1 and 2. The simulated data (bold symbols) match very well with the probabilistic Eq. (16) (thin line).

Secondly the ratio of fractal dimension  $\Delta_{P=f(A)}/\Delta_{A=f(P)}$  is computed for all the configurations and compared with our probabilistic approach (Eq. (16)) that confirms our prior hypothesis to obtain an analytical formulation. A statistical analysis (analysis of variance) shows that the number of islands used to calculate the perimeter and the area is the most relevant factor which affects the difference between probabilistic and simulation results. Four configurations with  $n = 10-100$  islands are considered in Fig. 2; it is shown that the coherence between the two approaches is quite good when the number of islands is higher than 50 notwithstanding a small bias for the lower values.

We then analysed the correlation  $\Delta_{a,s,\Delta_A,k,n=100,t}^{P=f(A)}$  and  $\Delta_{a,s,\Delta_A,k,n=100,t}^{A=f(P)}$  for a fractal dimension  $\Delta = 1$ . For this purpose,  $\Delta_{a=0.5,s,\Delta_A=2,k,n=100,t}^{P=f(A)}$  is plot versus  $\Delta_{a=0.5,s,\Delta_A=2,k,n=100,t}^{A=f(P)}$  (Fig. 3a) for  $n = 100$  simulations for

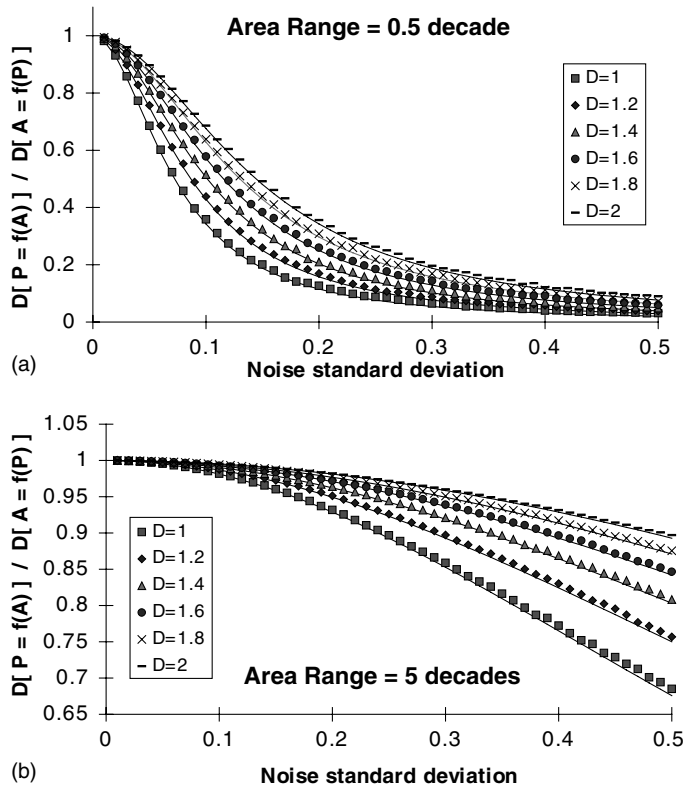


Fig. 1. Ratio of fractal dimension obtained by regression of  $P = f(A)$  on fractal dimension obtained by regression  $A = f(P)$  versus the experimental noise standard deviation of the perimeter measurement on the area measurement. These ratios are calculated by the probabilistic equation (16) (thin line) and by Monte-Carlo simulation (bold symbols are the means of 100 simulations). The number of decades for the area measurement is 0.5 (a) or 5 (b).

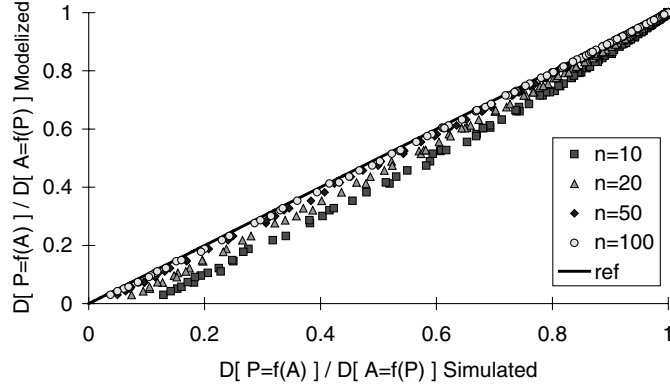


Fig. 2. Comparison between ratio of the fractal dimension calculated by  $P = f(A)$  on  $A = f(P)$ . In ordinate, the ratio is obtained by Eq. (16) and in abscissa by the Monte-Carlo simulation. All configurations of the set  $\aleph$  are considered and statistical analysis shows that the parameter “number of islands” gives the biggest difference between analytical and Monte-Carlo models. The symbols are related to the four sets of data ( $n = 10, \dots, 100$  islands) and the line represents a perfect correlation between the two models.

each different noise varying between 0.05 and 0.5. After linear regression, the slope between the two regressions is plotted versus the experimental noise,  $s$ , in Fig. 3b.

These surprising results can be shown:

- (i) The slope decreases when the noise rises according to Eq. (16). For low noise, the correlation coefficient  $r$  tends towards 1 and both Eqs. (3) and (8) give the same fractal dimension. For noises higher than 0.3 the slope becomes negative that cannot be accounted for Eq. (16). This equation assumes that the standard deviation for the noise is perfectly known and is not a random variable. However, this standard deviation obeys a determined statistical law. By 100,000 Monte-Carlo simulations for  $s_e = 0.05$  (positive correlation),  $s_e = 0.3$  (zero correlation) and  $s_e = 0.5$  (negative correlation), it was shown that the slope does not depend on the number of data considered for the regression, but that the scatter decreases as the number of data rises. In other words, the negative correlation does not disappear when the number of islands rises.

For a noise lower than 0.3, if  $\Delta_{P=f(A)}$  rises, then  $\Delta_{A=f(P)}$  rises. When the noise becomes higher than this critical value then if  $\Delta_{P=f(A)}$  rises,  $\Delta_{A=f(P)}$  decreases. As a consequence, for a noise higher than a critical value, when a physical process is positively correlated with the fractal dimension calculated by mean of the regression  $\log(\textit{Perimeter})$  versus  $\log(\textit{Area})$ , then the same physical process is negatively correlated with the fractal dimension when the regression is performed on  $\log(\textit{Area})$  versus  $\log(\textit{Perimeter})$ . Some contradictions in literature are readily explained by this first result.

- (ii) The barycentre of each set of data corresponds to Eq. (16).
- (iii) The distribution of the data around the  $\Delta_{P=f(A)}$  is equal to 1. That is obvious since the Gauss–Markov hypotheses are verified for our simulation and therefore the fractal dimension calculated by the regression  $\log(\textit{Area})$  versus  $\log(\textit{Perimeter})$  is unbiased and has 1 as average value.

To calculate the correlation between the two representations, a master curve has to be determined by successive simulations. With that aim in view we consider both regression and variance analysis. To begin, all configurations  $\Pi_{a,s,\Delta_A,k,n=N,t}$  for  $N = \{10, 20, 50, 100, 500\}$  are simulated. Considering  $n$  higher than 50, it is possible to show that the slope only depends on the variable  $s_e/\Delta_a$  and on the fractal dimension. The master curves are determined by Monte-Carlo simulations on the entire domain  $\aleph$  (Fig. 4) supposing that the experimental work is performed with 50 islands whose surfaces vary within a two decades interval

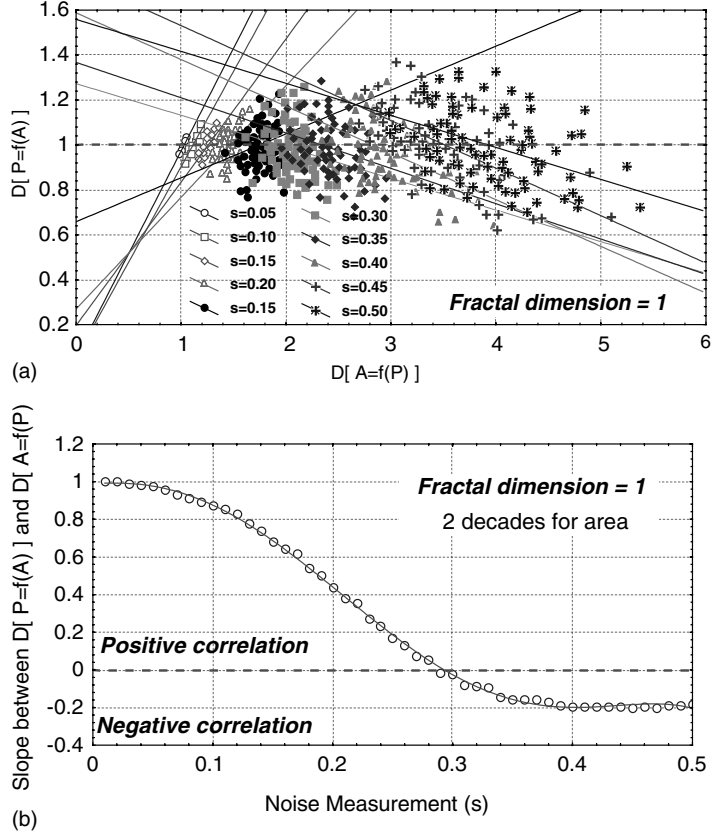


Fig. 3. (a) Monte-Carlo results  $\Delta_{a=0.5, s, \Delta_A=2, k, n=100, t}^{P=f(A)}$  versus  $\Delta_{a=0.5, s, \Delta_A=2, k, n=100, t}^{A=f(P)}$ , and (b) means of the ratio  $\Delta_{a=0.5, s, \Delta_A=2, k, n=100, t}^{P=f(A)}$  on  $\Delta_{a=0.5, s, \Delta_A=2, k, n=100, t}^{A=f(P)}$ , for 100 simulations with noise,  $s$ , varying between 0.05 and 0.5 for a fractal dimension  $\Delta = 1$  and two decades for area measurement. The sign of the correlation depends on the experimental noise.

( $\Delta_A = 2$ ) and a  $s_{e'} = 0.2$  standard deviation of the data versus the regression line. Two fractal dimensions are calculated with the two types of regression and the ratio  $\Delta_{P=f(A)}/\Delta_{A=f(P)} = 0.6$  with  $s_e/\Delta_a = 0.1$ . From Fig. 4, it can be inferred that the fractal dimension is 1.2 if the experimental noise  $s_{e'}$  is the same whatever the dimension of the island and without any noise in the area measurement.

### 3.2.5. Correlation between fractal dimension and physical process

In the above section, it was shown that a positive or a negative correlation might be found depending on the choice of the abscissa and ordinate. We now suppose that the fractal dimension is linearly well correlated with a physical property. We shall determine if the island method is appropriate to calculate the fractal dimension according to the representation  $A = f(P)$  or  $P = f(A)$ , the experimental noise and the correlation range. To this end, simulations are performed using the Monte-Carlo method.

Let the set of configurations be  $\mathfrak{N}_{a, s, \Delta_A, k, n, t}$ , with  $a_{\min} \in \{0.5, 0.6, \dots, 1\}$ ;

$$a \in \left\{ a_{\min} + \frac{0}{n_a} \Delta_a, a_{\min} + \frac{1}{n_a} \Delta_a, a_{\min} + \frac{2}{n_a} \Delta_a, \dots, a_{\min} + \frac{k_a}{n_a} \Delta_a, \dots, a_{\min} + \frac{n_a}{n_a} \Delta_a \right\};$$

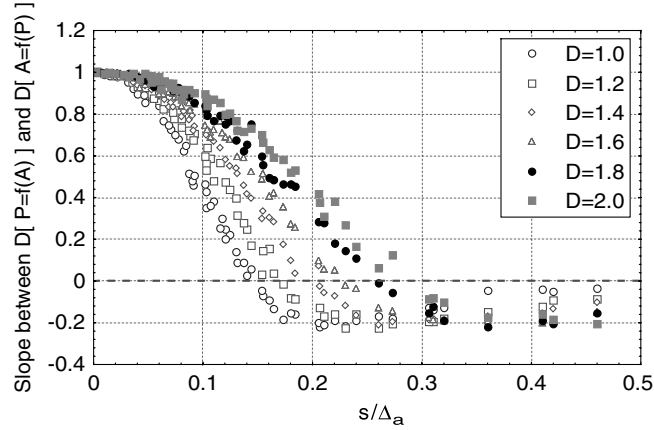


Fig. 4. Master curve of the slope between  $\Delta_{P=f(A)}$  and  $\Delta_{A=f(P)}$  versus the ratio  $s/\Delta_a$  for fractal dimension varying between 1 and 2. All Monte-Carlo configurations are considered.

$$\Delta_a \in \{0.1, 0.2, 0.5\}; s \in \{0.01, 0.02, \dots, 0.5\}; \Delta_A \in \{0.5, 0.1, \dots, 5\};$$

$$A \in \left\{ \frac{0}{n} \Delta_A, \frac{1}{n} \Delta_A, \frac{2}{n} \Delta_A, \dots, \frac{k}{n} \Delta_A, \dots, \frac{n}{n} \Delta_A \right\};$$

$n$  the number of points used for the regression,  $A$  the area,  $a$  the slope of  $\log P$  versus  $\log A$  and  $t$  the index of the simulation.

Eq. (8) is simulated in the following form:

*Stage 1:* All pairs area–perimeter contained in the configuration set are simulated (Fig. 5).

*Stage 2:* The fractal dimensions  $\Delta_{P=f(A)}$  and  $\Delta_{A=f(P)}$  are calculated for all pairs of stage 1 by the least square method (Fig. 6).

*Stage 3:* The regression  $\Delta_{P=f(A)}$  and  $\Delta_{A=f(P)}$  are performed for values belonging to the set  $a$ . If the noise is low enough, then  $\Delta_{P=f(A)} \approx \Delta_{A=f(P)} \approx 2a$ . The real fractal dimension is plotted in Fig. 7 versus the estimated

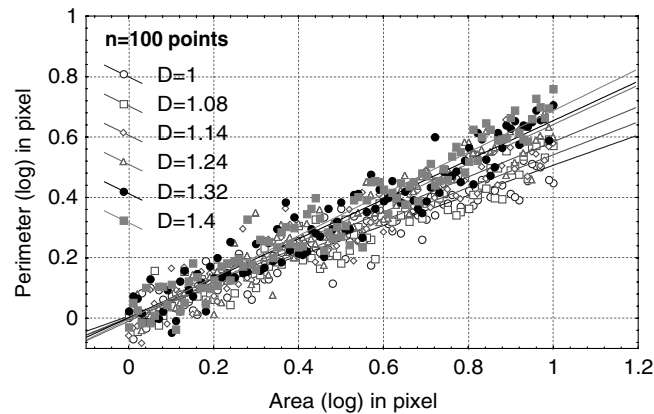


Fig. 5. First step of the Monte-Carlo algorithm: all pair  $\log(\text{Perimeter})$  versus  $\log(\text{Area})$  are simulated for fractal dimension varying between 1 and 1.4.

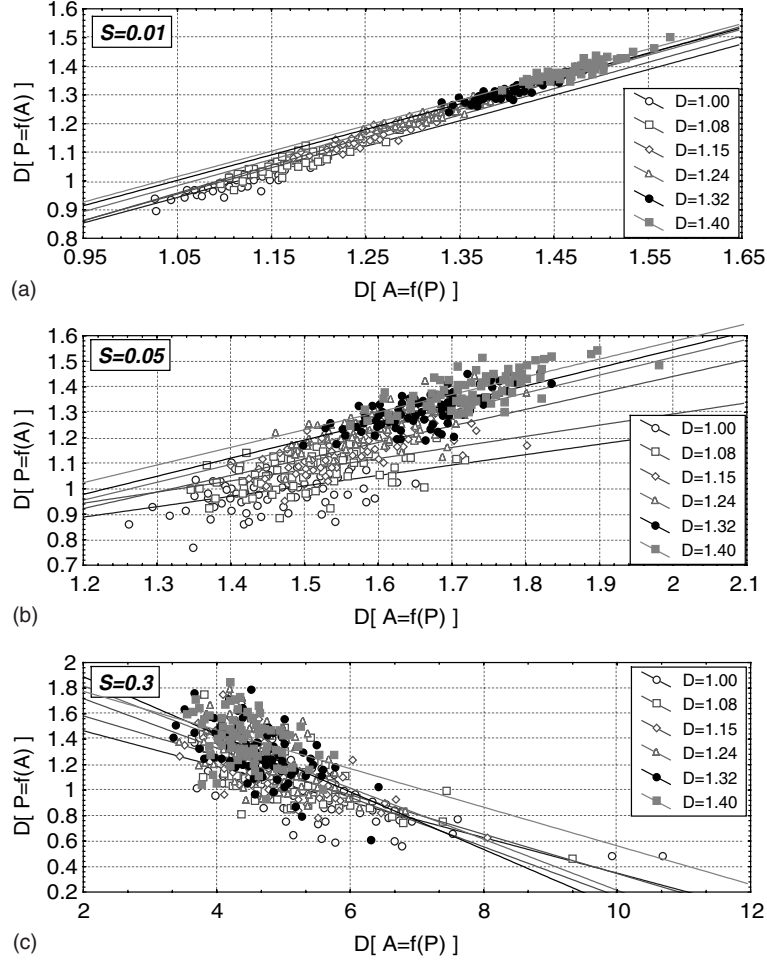


Fig. 6. Second step of the Monte-Carlo algorithm: The slope of  $\Delta_{P=f(A)}$  versus  $\Delta_{A=f(P)}$  is simulated for three values of the residual standard deviation of the area noise measurement (a)  $s_{\sigma'} = 0.01$ ; (b)  $s_{\sigma'} = 0.05$ ; and (c)  $s_{\sigma'} = 0.3$ .

fractal dimension for the two regression modes. Fig. 7 requires a physical explanation. The abscissa represents a fractal dimension varying between 1 and 1.4 and the ordinate the measure obtained by the regression of  $\log(\text{Perimeter})$  versus  $\log(\text{Area})$  on the left-hand side and  $\log(\text{Area})$  versus  $\log(\text{Perimeter})$  in the right-hand side of the graph. If the fractal dimension of the physical process rises linearly from 1 to 1.4 ( $a_{\min} = 0.5$ ,  $\Delta_a = 0.2$ ) and if the noise is low ( $s_{\sigma'} = 0.01$ ), then the two regressions give nearly the same slope and the representations  $\Delta_{P=f(A)}$  and  $\Delta_{A=f(P)}$  are equivalent. Considering now a higher noise ( $s_{\sigma'} = 0.2$ ) which corresponds to the experimental noise reported in literature, it can be shown that the correlation between the calculated and the theoretical fractal dimensions still holds for the first representation in spite of a rising scatter with the noise. On the contrary, if the regression is carried out on  $\log(A)$  versus  $\log(P)$  the slope is sometimes positive and sometimes negative. Consequently, the experimenter may find a downward trend in correlation of the fractal dimension with the physical process although the true correlation is positive. Worse than that, the classical statistic test might be significant.

*Stage 4:* Performance of the statistical calculation on the slope obtained in stage 3.

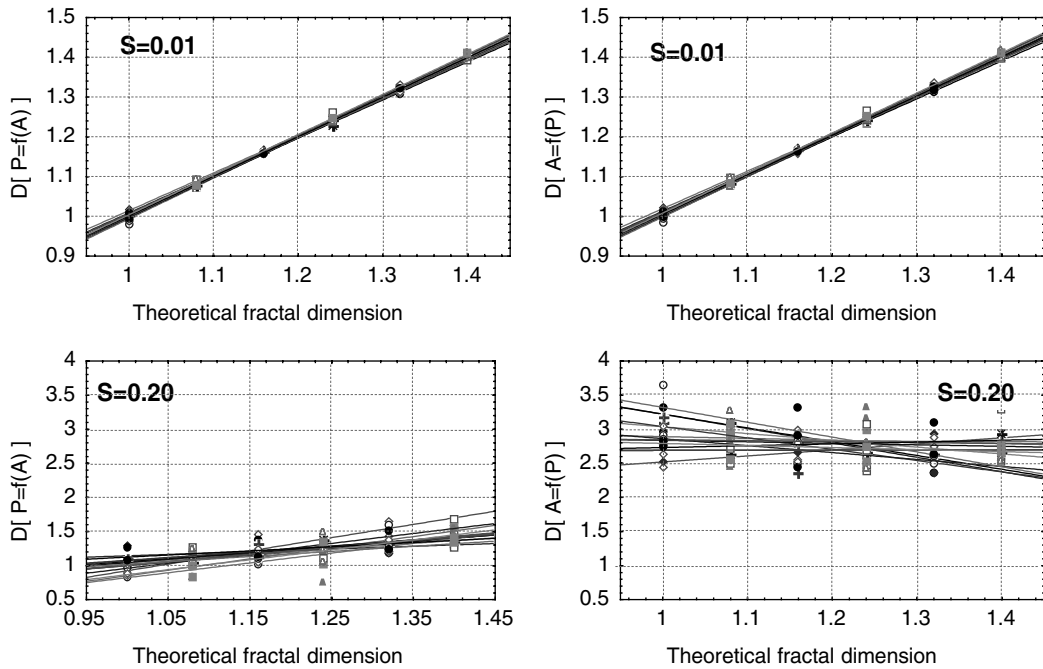


Fig. 7. Correlation between simulated and theoretical fractal dimension by regressing perimeter versus the area (left) or area versus perimeter (on the right). Three residual standard deviation ( $s_e = 0.01, 0.05, 0.2$ ) are considered. One line corresponds to a Monte-Carlo simulation.

The histograms in Fig. 8 represent the distribution of the slope for the two representations. It is shown that:

- (i) The scatter in the slope rises with  $s_e$ .
- (ii) The histograms are symmetrical for the  $\Delta_{P=f(A)}$  and seem Gaussian.
- (iii) The more the dispersion rises, and the more the distribution of  $\Delta_{A=f(P)}$  loses its Gaussian aspect.
- (iv) The values are not centred on 1 for  $\Delta_{A=f(P)}$  and this shift is higher when the noise residual standard deviation rises.

We now calculate the rank correlation instead of the statistic moments since they are not defined for calculating  $\Delta_{A=f(P)}$ . We only calculate the median and the 5% and 95% quantiles since they are always defined (Fig. 9).

*Stage 5:* The correlation diagram is plotted to answer the question: is the correlation  $\Delta_{A=f(P)}$  significant? As the indicator of correlation we have chosen is the median, we shall use two parametric statistical tests (rank and sign test). The critical probability we plot in ordinate is the probability that we wrongly state by the median equals zero, i.e. the correlation between the fractal dimension and the physical process does not exist. As usual, the threshold 0.05 is considered. The graphs have been plotted (Fig. 10) for the two types of representation. It can easily be shown that the correlation becomes insignificant (95% confidence interval) if the noise residual standard deviation varies between 0.16 and 0.18. If  $s_e < 0.16$ , the correlation is positive and if  $s_e > 0.18$ , it is negative.

In other words, if a physical process is perfectly positively correlated with the fractal dimension which varies between 1 and 1.4, then the experimenter who uses the representation  $A = f(P)$ , may find according

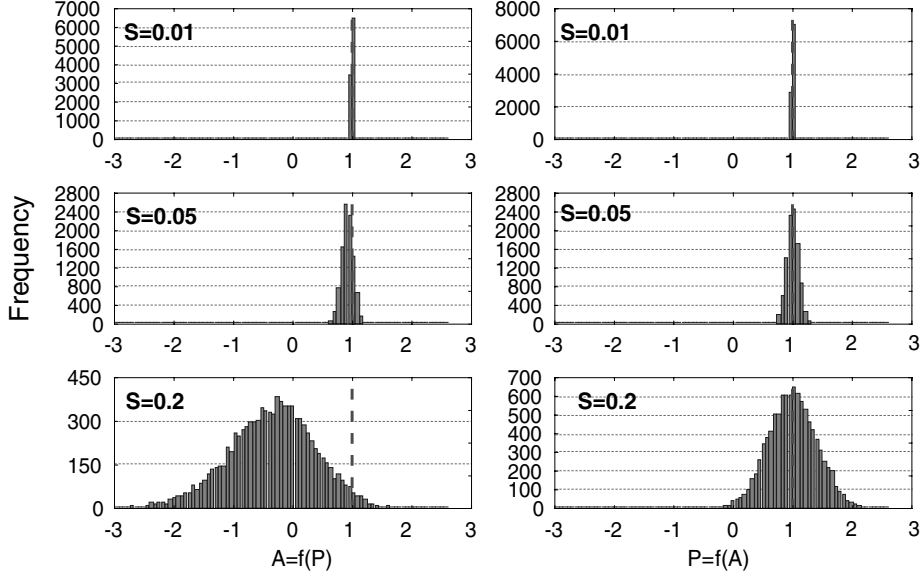


Fig. 8. Histograms of the slope between simulated versus calculated fractal dimensions obtained for 10,000. Monte-Carlo simulations and a residual standard deviation on the area or perimeter measurement  $s_e = 0.01, 0.05, 0.2$ . Right are the results for the  $P = f(A)$  regression and left for  $A = f(P)$ .

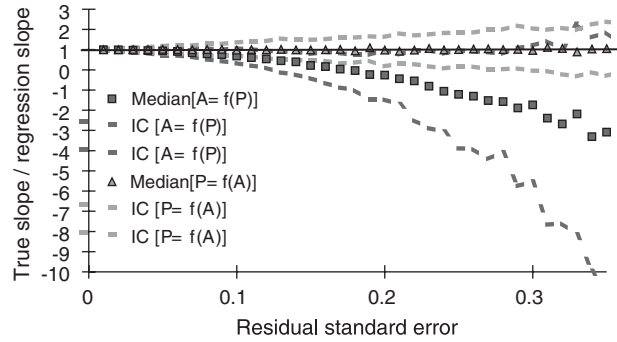


Fig. 9. No-parametrical statistic analysis of the histograms in Fig. 8. IC represents the 95% confidence interval.

to the experimental error ( $s_e$ ) if the correlation is positive, negative, or does not exist. If the representation  $P = f(A)$  is preferred, he will always obtain a positive correlation. Nevertheless, this numerical application with mean values chosen among the results coming from the literature depends on  $a_{\min}$ ,  $A_a$ ,  $A_A$ . This simulation has to be extended to all the configurations of the simulation set, and after calculation it has been shown [42] that the median can be modelled by the following equations:

$$Med^{A=f(P)} = 1 - 72_{\pm 6} [1 - 0.91_{\pm 0.004} a_{\min} - 0.42_{\pm 0.006} A_a] \left[ \frac{s_e}{A_A} \right]^{2 \pm 0.02} \quad (17)$$

$$Med^{P=f(A)} = 1 \quad (18)$$



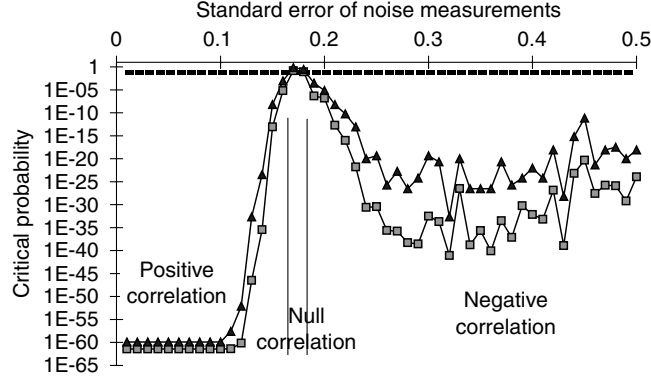


Fig. 10. Critical probability versus the experimental noise for the two type of regression (a)  $A = f(P)$  and (b)  $P = f(A)$ . The data are related to the configuration:  $a \in \{0.5\}$ ;  $\Delta_a \in \{0.2\}$ ;  $\Delta_A \in \{1\}$ , and  $n = 100$ .

Eqs. (17) and (18) represent the influence of the abscissa and ordinate chosen for the SIM representation on the correlation under the assumption that a uniform noise affects only the measurement of the perimeter.

To summarise the physical aspect of this development we consider a relation between the fractal dimension and the fracture toughness such that  $K_{IC} = 50\Delta$ . The fractal dimension varies from 1 to 1.4 ( $a_{\min} = 0.5$ ,  $\Delta_a = 0.2$ ) the standard deviation in the perimeter determination is  $0.2 \mu\text{m}$  ( $s_p = 0.2$ ) and the area is measured on 1 decade ( $\Delta_A = 0.2$ ). We find  $Med^{A=f(P)} = -0.32$ , and a 50% probability that the correlation is negative by regressing area versus perimeter.

#### 4. Application and discussion

It was shown that the relation between the theoretical and the experimental fractal dimension  $\Delta_{P=f(A)}$  is unbiased if there is no noise when recording the area. Only the amplitude of the experimental noise, a low range for the area variation, a low variation between  $\Delta$  and the physical process or a reduced number of recorded islands prevent from calculating the precise fractal dimension. If a relation is found, then this relation has a physical signification.

To test whether the experimental noise has an effect on the result, we now simulate the fractal dimension by a Monte-Carlo algorithm and the bias obtained by regression  $A = f(P)$  and  $P = f(A)$  by considering  $s_P$  and  $s_A$  the standard deviation for the perimeter and the area respectively. We also propose a new method to perform the regression by minimising the orthogonal distance between experimental data and the slope (principal component analysis) instead of vertical or horizontal distance. This method is rather difficult to compute since the eigenvalues have to be calculated. However it gives a fractal dimension which is independent of the type of representation  $A = f(P)$  or  $P = f(A)$ .

Three limited cases are considered in Fig. 11:

- (i) Noise is introduced only on the perimeter measurement.
- (ii) Noise is introduced on both perimeter and area measurement.
- (iii) Noise is introduced only on the area measurement.

From Fig. 11, it can be inferred:

- (i)  $\Delta_{P=f(A)}$  is unbiased since the area is recorded without any noise.
- (ii)  $\Delta_{A=f(P)}$  is unbiased since the perimeter is recorded without any noise.

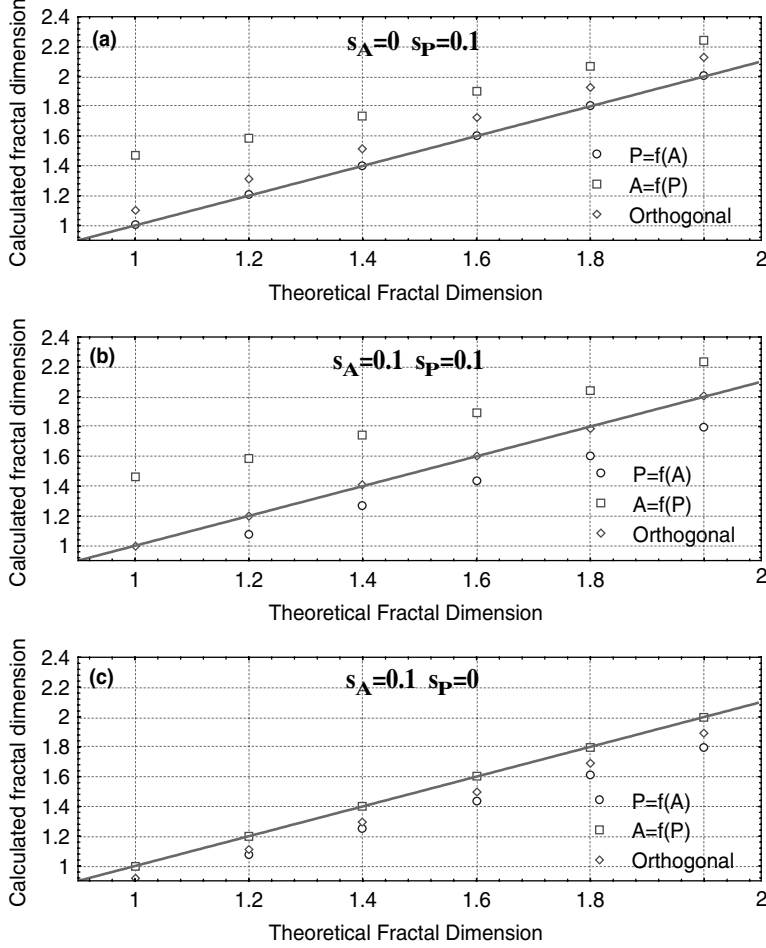


Fig. 11. Fractal analysis with the three regressions:  $A = f(P)$ ,  $P = f(A)$  and orthogonal.  $s_A$  and  $s_P$  represent respectively the noise on area and perimeter measurements. The symbols represent the average of 100 Monte-Carlo simulations with  $\Delta_A \in \{0.5, 0.1, \dots, 5\}$  and a number of data 50, 250 and 450. The line represents the perfect relation between the theoretical and the calculated fractal dimensions and is given as guidelines for the eyes.

- (iii) The orthogonal regression is unbiased if the perimeter and area scatter is of the same order of magnitude.
- (iv) The  $\Delta_{A=f(P)}$  bias rises with the fractal dimension, accordingly to Eq. (12).
- (v) The  $\Delta_{A=f(P)}$  bias is higher than the  $\Delta_{P=f(A)}$  bias if the uncertainty on the perimeter and area determinations is of the same order of magnitude.
- (vi) The fractal dimension calculated by the orthogonal method lies between the two other results.

We then compute the fractal dimension by considering  $s_P$  and  $s_A$  the standard deviations for the perimeter and the area. We must first quantify the error made by the representation  $\Delta_{P=f(A)}$  with a noise  $s_A$  which violates the Gauss–Markov hypothesis. After calculations, it can be shown that:

$$Bias_{P=f(A)} = 3.3_{\pm 0.01} \Delta \left( \frac{s_A}{\Delta_A} \right)^{1.5_{\pm 0.0015}} \quad (19)$$

This relation model the error made on the fractal dimension with a  $\pm 0.03_{95\%}$  uncertainty. It can be shown that the bias is independent of both the number of islands considered and the standard deviation.

The same process gives a negative bias considering the  $\Delta_{A=f(P)}$  representation:

$$Bias_{A=f(P)} = -51.12_{\pm 0.12} \frac{1}{\Delta} \left( \frac{s_P}{\Delta_P} \right)^{2.04_{\pm 0.0013}} \quad (20)$$

From these equations, it is shown that an increasing noise on the area measurement induces a decreasing calculated fractal dimension. In the same way, the fractal dimension becomes higher if the number of decade rises.

By non-linear regression, the orthogonal representation induces the following bias:

$$Bias_{Ortho} = 1.29_{\pm 0.11} \Delta \left( \frac{s_P}{\Delta_P} \right) \left( \frac{s_A}{\Delta_A} \right) - 19.6_{\pm 0.26} \left( \frac{s_P}{\Delta_P} \right)^{2.15_{\pm 0.01}} + 5.93_{\pm 0.17} \left( \frac{s_P}{\Delta_P} \right)^{1.91_{\pm 0.02}} + 6.08_{\pm 0.8} \left( \frac{s_P}{\Delta_P} \right) \left( \frac{s_A}{\Delta_A} \right) \quad (21)$$

These three preceding equations allow us to calculate the error made on the fractal dimension by using the slit island method if the standard deviations on the perimeter and area measurement are known.

To test the efficiency of (19)–(21) we draw in Fig. 12 the modelled errors related to our experimental values. It is obvious that:

- (i) Our models well represent statistical errors in the SIM.
- (ii) It avoids using the  $A = f(P)$  representation since the bias is too important, moreover it is always negative and gives a fractal dimension higher than the true one.
- (iii) Using the  $P = f(A)$  relation always leads to a positive bias. That means that the calculated fractal dimension is always less than the true one. That might explain why Ray et al. found a negative fractal dimension using that representation [6].
- (iv) Choice of orthogonal or  $P = f(A)$  regression depends on the formula which minimise the statistical bias.

Moreover Eqs. (19)–(21) give possible explanations for negative or positive relationship reported between fractal the dimension and mechanical properties.

As an example of the use of these relations we consider the two following cases supposing that no relations exists between the fractal dimension and MP.

A negative correlation can be found by regressing perimeter versus the area if:

- (i) The standard deviation in the area measurement is more important when MP increases.
- (ii) The number of decades rises when MP becomes higher.

A positive correlation can be found if:

- (i) The perimeter standard deviation is higher when MP increases.
- (ii) The number of decade decreases with MP.

This conclusion is not only a theoretical case with no probability to occur. Literature results show that the island morphology (area, shape . . .) evolves with mechanical properties and then an erroneous correlation can be found with  $s_A/\Delta_A$  (in Eq. (19)) or  $s_P/\Delta_P$  (in Eq. (20)).

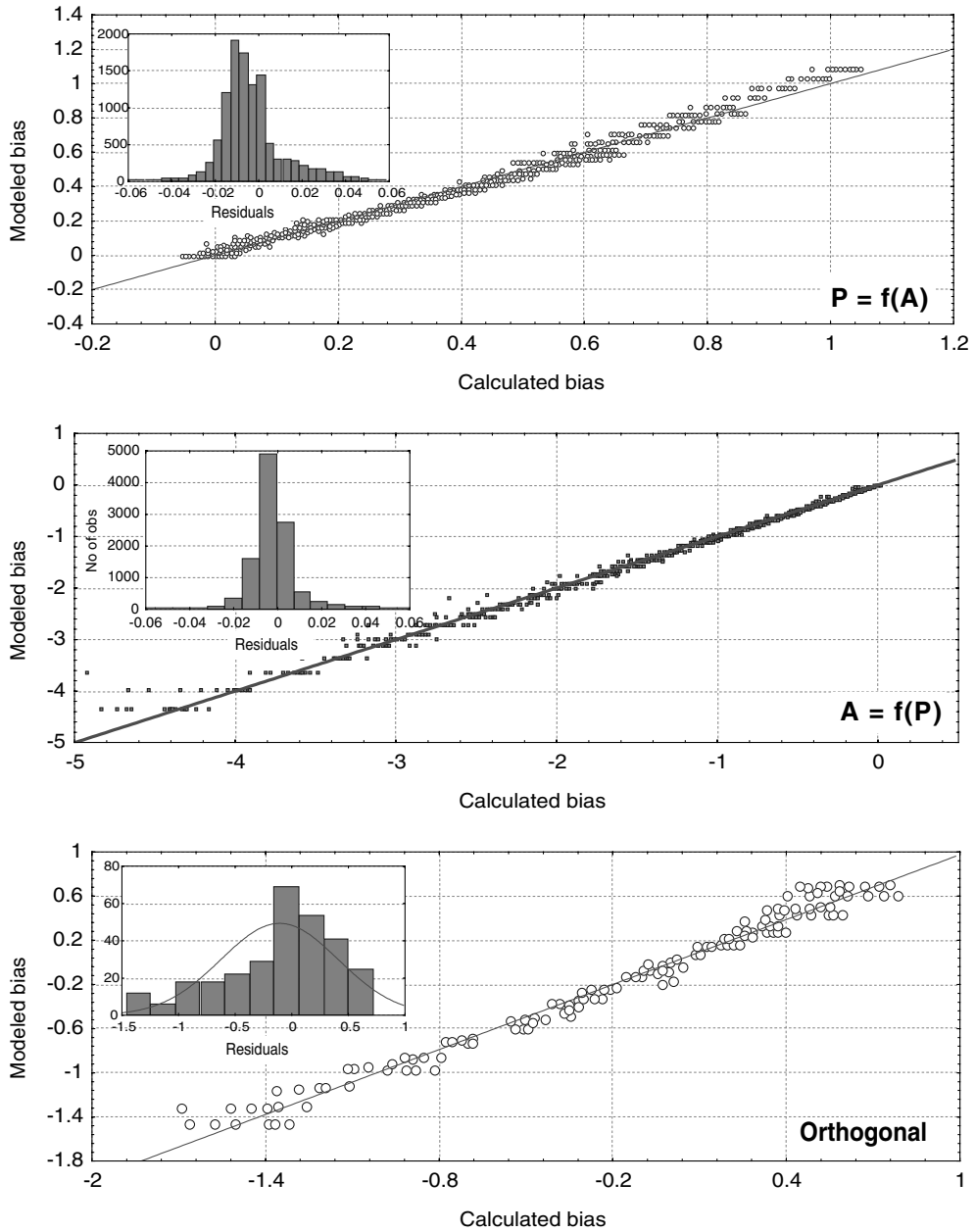


Fig. 12. Comparison of modelled and simulated bias obtained for the three representations  $P = f(A)$  (Eq. (19)),  $A = f(P)$  (Eq. (20)) and orthogonal (Eq. (21)).

We search in the literature results containing sufficient information to carry out statistical simulations about the variation of the fractal dimension of fractured surface in relation with mechanical properties. It was found that:

- (i) The scatter in area and perimeter measurements are always the same, respectively 0.15 (with a standard deviation of  $\sigma = 0.05$ ) and of 0.11 ( $\sigma = 0.07$ ) which is statistically equivalent (Student test for results reported in Table 1).
- (ii) Residuals obtained for area perimeter representation are Gaussian.
- (iii) Many errors are made on the calculation of the fractal dimension.

As a consequence, it is difficult to state if positive or negative correlation can be deduced from the literature results between the fractal dimension and mechanical properties (or other physical processes) since the experimental noise introduces artefacts both in calculation of the fractal dimension and in the correlation.

Many researchers have tried to correlate the fractal dimension with mechanical properties such as impact energy and fracture toughness from the observation of surface of the fracture. Some researchers report the validity of the fractal analysis but other researchers report the converse results. The main reason for the discrepancy is that the actual fracture mechanisms and processes are very complex and not so ideal for the fractal analysis to be easily applied. In some cases, different mechanisms control the fracture and the linear relation is not obtained on log–log plots of data obtained from mechanical tests with a wide range of test temperatures, heat treatment, etc. We have proposed a statistical reason for the discrepancy. However, we have supposed that data perfectly obeys the Gauss–Markov hypotheses that will be false if the linear relation is rejected. What will our conclusion be if data violate the linear relation? Firstly, if the linear relation is rejected then the fractal dimension cannot be estimated formally. However it is sure that a low deviation from the linear relation can be observed without systematically rejecting the fractal concept. In this case, what will be the evaluation of the fractal dimension? Does a statistical artefact then appear?

To appreciate this possible artefact, one has to introduce a non-pure linear relation characterizing the usual non-linear representation met in the bibliography.

$$P = 0.75\theta A + e(\log A - \alpha(\theta, e)) \quad (22)$$

where  $\alpha(\theta, e)$  is calculated such that the fractal dimension  $2 * 0.75\theta A$  will be calculated without bias by the least square regression using the  $P = f(A)$  representation.  $P = 0.75\theta A + e(\log A - \alpha(\theta, e))$  is an amplified factor of the non-linearity and  $\theta$  is a variable that will change the fractal dimension.

Fig. 13 represents the log–log graph for different  $e$  values and  $\theta = 1$ . We have then calculated the value of the fractal dimension by the representation  $A = f(P)$ . We obtained the following results:

- For any fixed  $e$ , if  $\theta$  increases (respectively decreases), then the fractal dimension  $\Delta_{A=f(P)}$  increases (respectively decreases): If  $\theta$  is a physical parameter that modifies the fractal dimension, a constant change of linearity does not affect this tendency and then no false correlation is introduced (see Fig. 14).
- The non-linearity does not really change the results we present in this article about the influence of the statistical noise on the area and perimeter measurement on the fractal dimension.
- The fractal dimension depends on the  $e$  values. Fig. 15 represents the effect of the non-linearity on  $\Delta_{A=f(P)}$ . If non-linearity increases, the calculated fractal dimension decreases: it is an important fact because if fracture mechanisms or processes involve a monotonous change with a physical parameter (for example test temperature, heat treatment) then a correlation can be found between the mechanical properties and the fractal dimension even if no correlation exists. However, all simulations we have carried out seem to converge to the opinion that non-linearity will not affected the determination of the fractal dimension by a factor higher than 0.02 (see Fig. 15).

However, to us whatever the representation used, the highest artefact could result from the change of  $s_A$ ,  $\Delta_A$ ,  $s_P$  or  $\Delta_P$  with the physical process according to Eqs. (19)–(21). Let us illustrate the example met in the bibliography [44] to which we can apply our results. Using the  $\Delta_{P=f(A)}$  relationship, Su et al. [44] find

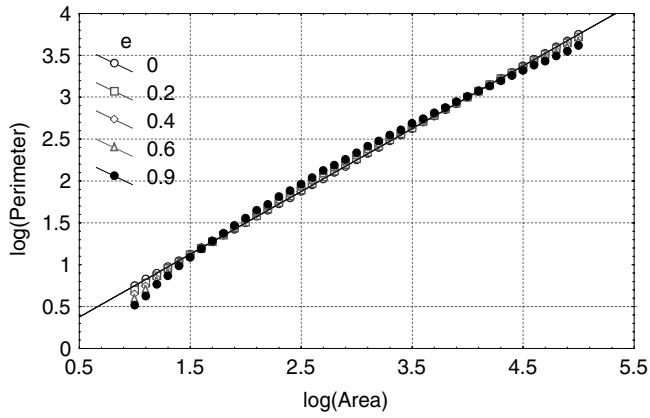


Fig. 13. Log-log graph perimeter–area relation for different  $e$  values such that  $P = 0.75A + e(\log A - \alpha(1, e))$ .

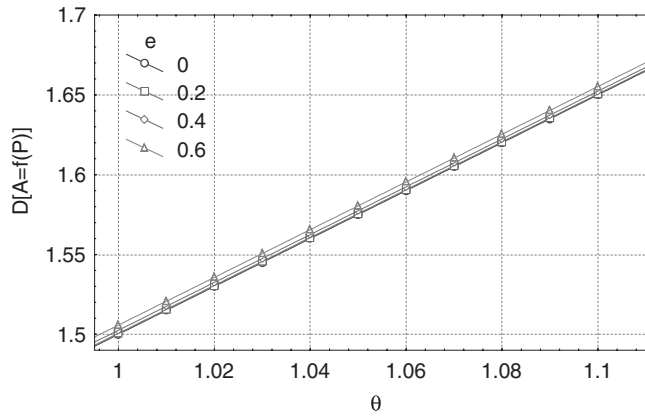


Fig. 14. Evolution of  $\Delta_{A=f(P)}$  with a physical parameter  $\theta$  given by Eq. (22) with different  $e$  values.

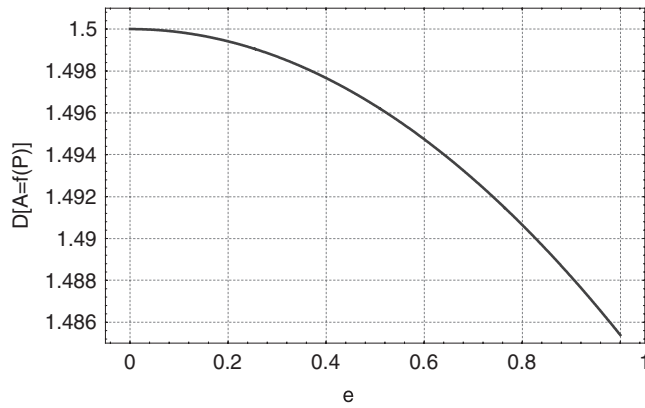


Fig. 15. Effect of the non-linearity factor  $e$  for  $\theta = 1$  on the estimation of the fractal dimension  $\Delta_{A=f(P)}$ .

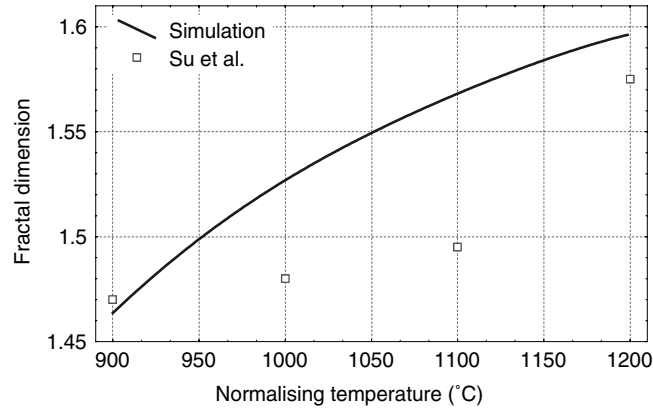


Fig. 16. Effect of the bias introduced by the Slit Island Method when fractal dimension stays unchanged and equals 1.7 (thin line) and experimental data given by Su et al.

that the fractal dimension of pearlite in HSLA steel increases from 1.47 to 1.57 with different normalizing temperatures (900–1200 °C). The higher normalizing temperature, the higher the pearlite area (increases of the radius size from 20 to 50  $\mu\text{m}$  quasi-linearly). This means that  $\Delta_A$  will double and according to Eq. (19) with supposing  $s_A$  constant introduced a relation of bias of to 0.03–0.09. We have simulated under the condition given by Su et al. supposing that the fractal dimension does not depend on the normalizing time and equals 1.7, the fractal dimension calculation versus the normalizing time and reported their results. As can be observed in Fig. 16, even if the fractal dimension does not change with the normalizing time, an increasing tendency of fractal dimension with the normalizing time is found near the relation obtained by Su et al. and only due to the statistical bias introduced by the SIM. That does not mean that the relation claimed by the authors does not exist but simply means that the bias will emphases this relation.

## 5. Conclusion

Statistical analysis and simulation have been used to study the fractal dimension calculated by the SIM. The analysis shows that the results depend on the choice of ordinates and abscissa chosen for the area and the perimeter. If there is no noise on the area, then the representation  $P = f(A)$  gives a correct value of  $\Delta$ . If an experimental noise exists on the perimeter, the regression  $A = f(P)$  gives erroneous value for  $\Delta$ , especially if the perimeter range decreases and the noise becomes more important. For this case, the calculated fractal dimension is higher than the true one. If the measurement is of the same order of magnitude as far as area and perimeter are concerned, then the new orthogonal method we proposed is more suitable to calculate  $\Delta$ .

Finally, it was shown that the SIM might produce artefacts in the correlation between fractal dimension and a physical process, and that some results in literature should be considered with much caution.

The main defect of the SIM is its lack of statistical robustness to study the fractal dimension related to a physical process. Some other artefacts can occur to modify the information measurement during image acquisition (focusing, threshold, magnification, brightness . . .) and give erroneous results. Moreover, the authors who used the classical statistical test for linear regression in log–log co-ordinates give a fractal dimension  $\Delta = \alpha \pm \beta$ . The uncertainty  $\beta$  is generally low, but this method supposes that the Gauss–Markov

hypotheses are verified, and we have shown that current statistics can give false values. Consequently, the attempt to correlate the fractal dimension with a physical process first requires a good unbiased estimation of  $\Delta$ .

### Acknowledgement

We wish to thank Véronique Hague for her assistance in English.

### Appendix A

The  $T$  truncated Gaussian law is defined by:

$$\varphi(t) = \frac{f(t)}{2F(t) - 1} \quad \text{for } -T \leq t \leq T \quad (\text{A.1})$$

and  $\varphi(t) = 0$  elsewhere with

$$f(t) = \frac{1}{\sqrt{2\pi}} \exp\left(-\frac{t^2}{2}\right) \quad \text{and} \quad F(X) = \int_{-\infty}^X f(t) dt$$

The moments (null for  $k$  odd) are estimated by:

$$\mu_k = \int_{-T}^T t \varphi(t) dt = (k-1)\mu_{k-2} - \frac{2f(T)}{2F(T) - 1} T^{k-1} \quad (\text{A.2})$$

As  $\mu_0 = 1$ , Eq. (A.2) can be written thanks to an expansion as:

$$\mu_k = 1.3 \dots (k-1) \left( 1 - \frac{2f(T)}{2F(T) - 1} \left( T + \frac{T^3}{3} + \frac{T^5}{3.5} + \dots + \frac{T^{k-1}}{3.5 \dots (k-1)} \right) \right)$$

However

$$\frac{2f(T)}{2F(T) - 1} = \left( T + \frac{T^3}{3} + \frac{T^5}{3.5} + \dots \right)$$

and then:

$$\mu_k = \frac{2f(T)}{2F(T) - 1} \frac{T^{k+1}}{(k+1)} \left( 1 + \frac{T^2}{k+3} + \frac{T^4}{(k+3)(k+5)} + \dots \right)$$

To converge we must have:

$$\lim_{k \rightarrow \infty} \frac{\mu_{k+2}}{\mu_k} < 1 \quad \text{and} \quad \lim_{k \rightarrow \infty} \frac{\mu_{k+2}}{\mu_k} < T^2 \quad (\text{A.3})$$

Then  $T < 1$ .

Eq. (10) converges if:

$$\lim_{k \rightarrow \infty} \frac{\left(\frac{\sigma_\alpha}{\bar{\alpha}}\right)^{k+2} \mu_{k+2}}{\left(\frac{\sigma_\alpha}{\bar{\alpha}}\right)^k \mu_k} = \left(\frac{\sigma_\alpha}{\bar{\alpha}}\right)^2 \lim_{k \rightarrow \infty} \frac{\mu_{k+2}}{\mu_k} < 1 \quad (\text{A.4})$$



Then from Eq. (A.3), Eq. (A.4) will converge if the reduced centred Gaussian

$$x = \frac{\frac{2}{\Delta A=f(P)} - \bar{\alpha}}{\sigma_x}$$

is truncated by the  $T$  variable under condition given by Eq. (A.3) and then including Eq. (A.4), we get the convergence if  $(\sigma_x/\bar{\alpha})^2 T^2 < 1$ .

## References

- [1] Mandelbrot BB. Les objets fractals: forme, hasard et dimension. Paris: Flammarion; 1975.
- [2] Mandelbrot BB. The fractal geometry of nature. New York: W.H. Freeman; 1983.
- [3] Bouchaud E, Lapasset G, Planees J, Naveos S. Statistic of branched fracture surfaces. Phys Rev B 1993;48(5):2917–28.
- [4] Bouchaud JP, Bouchaud E, Lapasset G, Planes J. Models of fractal cracks. Phys Rev Lett 1993;71(14):2240–3.
- [5] Saouma VE, Barton C. Fractals, fractures, and size effects in concrete. J Engng Mech 1994;120(4):835–54.
- [6] Ray KK, Mandal G. Study of correlation between fractal dimension and impact energy in a high strength low alloy steel. Acta Metall Mater 1992;40(3):463–9.
- [7] Weisheng L, Bingsen C. Discussion on “the fractal effect of irregularity of crack branching on the fracture toughness of brittle materials” by Xie Heping. Int J Fract R 1994;R65–70.
- [8] Wang ZG, Chen DL, Jiang XX, Ai SH, Shih CH. Relationship between fractal dimension and fatigue threshold value in dual-phase steels. Scripta Met 1988;22:827–32.
- [9] Charkaluk E, Bigerelle M, Iost A. Fractal and rupture. Engng Fract Mech 1998;61(1):119–39.
- [10] Tanaka M. Fracture toughness and crack morphology in indentation fracture of brittle materials. J Mater Sci 1996;31:749–55.
- [11] Mecholsky JJ, Passoja DE, Feinberg-Ringel KS. Quantitative analysis of brittle fracture surfaces using fractal geometry. J Am Ceram Soc 1989;72(1):60–5.
- [12] Mecholsky JJ, Mackin TJ. Fractal analysis of fracture in Ocala chert. J Mater Sci Lett 1988;7:1145–7.
- [13] Lange DA, Jennings HM, Shah SP. Analysis of surface roughness using confocal microscopy. J Mater Sci 1993;28:3879–84.
- [14] Mandelbrot BB, Passoja DE, Paullay AJ. Fractal character of fracture surfaces of metals. Nature 1984;308:721–2.
- [15] Su H, Zhang Y, Yan Z. Fractal analysis of microstructures and properties in ferrite–martensite steels. Scripta Metall Mater 1991;25:651–4.
- [16] Lin G, Lai JKL. Fractal characterization of fracture surfaces in a resin-based composite. J Mater Sci Lett 1993;12:470–2.
- [17] Saouma VE, Barton C. Fractal characterization of fractured surfaces in concrete. J Engng Fract Mech 1990;35:47–53.
- [18] Pande CS, Richards LE, Louat N, Dempsey BD, Schwoeble AJ. Fractal characterization of fractured surfaces. Acta Met 1987;35(7):1633–7.
- [19] Richards LE, Dempsey BD. Fractal characterization of fractured surfaces in Ti–4.5Al–5.0Mo–1.5Cr (CORONA 5). Scripta Met 1988;22:687–9.
- [20] Brandt AM, Prokopski G. On the fractal dimension of fracture surfaces of concrete elements. J Mater Sci 1993;28:4762–6.
- [21] Bouchaud E, Lapasset G, Planes J. Fractal dimension of fractured surfaces: a universal value? Europhys Lett 1990;13(1):73–9.
- [22] Underwood EE, Banerji K. Fractals in fractography. Mater Sci Engng A 1986;80:1–14.
- [23] Mandelbrot BB. How long is the coast of Britain? Statistical self-similarity and fractal dimension. Science 1967;155:636.
- [24] Minkowski H. Über die Begriffe Länge, Oberfläche und Volumen. Deut Math 1901;Jahr9:115–21.
- [25] Tricot C. Courbes et dimension fractale. Paris: Springer-Verlag; 1993.
- [26] Dubuc B, Quiniou JF, Roques-Carnes C, Tricot C, Zucker SW. Evaluating the fractal dimension of profiles. Phys Rev A 1989;39(3):1500–12.
- [27] Ganti S, Busham B. Generalized fractal analysis and its applications to engineering surfaces. Wear 1995;180:17–34.
- [28] Lovejoy S. Area–perimeter relation for rain and cloud areas. Science 1982;216:185–7.
- [29] Elias H, Schwartz D. Surface areas of the cerebral cortex of mammals. Science 1969;166:111–3.
- [30] Weibel ER. Morphometry of the human lung. New York: Academic Press; 1963.
- [31] Hack JT. Studies of longitudinal streams in Virginia and Maryland. US Geological Survey Professional Papers, vol. 294B, 1957.
- [32] Huang ZH, Tian JF, Wang ZG. A study of the slit island analysis as a method for measuring fractal dimension of fractured surface. Scripta Metall Mater 1990;24:967–72.
- [33] Mc-Anulty P, Meisel LV, Cote PJ. Hyperbolic distributions and fractal character of fracture surfaces. Phys Rev A 1992;46(6):3523–6.
- [34] Imre A. Problems of measuring the fractal dimension by the slit-island method. Scripta Metall Mater 1992;27:1713–6.

- [35] Imre A. Comment on “perimeter-maximum-diameter” method for measuring the fractal dimension of a fracture surface. *Phys Rev B* 1995;51(22):16470.
- [36] Mu ZQ, Lung CW, Kang Y, Long Q. Perimeter-maximum method for measuring the fractal dimension of a fractured surface. *Phys Rev B* 1993;48(10):7679–81.
- [37] Chen Z, Mecholsky JJ, Joseph T, Beatty CL. The fractal geometry of Si<sub>3</sub>N<sub>4</sub> wear and fracture surfaces. *J Mater Sci* 1997;32:6317–23.
- [38] Lung CW, Mu ZQ. Fractal dimension measured with perimeter–area relation and toughness of materials. *Phys Rev B* 1988;38(16):11781–4.
- [39] Lung CW, Zhang SZ. Fractal dimension of the fractured surface of materials. *Physica D* 1989;38:242–5.
- [40] Meisel LV. Perimeter–area analysis, the slit-island method and the fractal characterization of metallic fracture surfaces. *J Phys D: Appl Phys* 1991;24:942–52.
- [41] Bigerelle M, Iost A. Analysis of the Koch island perimeter by the Richardson method. Monte-Carlo application to grain boundaries evolution during heating, in press.
- [42] Bigerelle M. PhD thesis, Caractérisation géométrique des surfaces et interfaces, applications en métallurgie. ENSAM Lille, 1999.
- [43] Schneider JM, Bigerelle M, Iost A. Statistical analysis of the Vickers hardness. *Mat Sci Eng A* 1999;262:256–63.
- [44] Su H, Yan Z, Stanley JT. Fractal analysis of microstructure and properties of HSLA steels. *J Mater Sci Lett* 1995;14:1436–9.
- [45] Pande CS, Richards LR, Smith S. Fractal characteristics of fractured surfaces. *J Mater Sci Lett* 1987;6:295–7.